



Implementation of four-port MIMO diversity microstrip antenna with suppressed mutual coupling and cross-polarized radiations

Sandeep Sharma^{1,3} · Mainuddin¹ · Binod Kumar Kanaujia² · Mukesh Kumar Khandelwal³

Received: 25 July 2019 / Accepted: 1 August 2019 / Published online: 6 August 2019
© Springer-Verlag GmbH Germany, part of Springer Nature 2019

Abstract

A compact four-element MIMO microstrip antenna is designed, analyzed and proposed for high frequency modern wireless applications. Proposed antenna is compact in size and offers a frequency band of about 6 GHz ranging from 23 to 29 GHz with a peak gain of 7.1 dBi and suppressed mutual coupling and cross-polarization level. Presented antenna possess better diversity with minimum mutual coupling among its all four elements. Diversity is verified in terms of envelope correlation coefficient, directive gain, total active reflection coefficient and ratio of mean effective gain. All the diversity parameters are found within the appropriate limit standardized for a MIMO device. Experimental results of fabricated prototypes verified the proposed results.

1 Introduction

In the present scenario, no one can imagine a life without mobile phone which has touched our lives up to deep rooted level and with time there is an increasing demand for infinite bandwidth along with enormous data rate. So, researchers and innovators are constantly looking forward for a technique that can cope up with the hunger of this everlasting demand of channel capacity. Now multiple input multiple output (MIMO) technology is one of the major advancements that can give a hope in this challenging situation.

Wallace (Wallace et al. 2003) suggested that multiple input multiple output (MIMO) techniques can be used to

enhance the channel capacity with no requirement of additional power because of its ability to transmit data over multiple channels. Furthermore, using MIMO systems pattern and polarization diversity can be achieved along with making the multipath fading less severe (Kaiser et al. 2009; Wang et al. 2009). Designing of MIMO antennas really takes a toll on the parts of researchers as there are several issues which are to be taken care of while designing. For an efficient MIMO antenna system, there are few performance matrices which are required in addition to regular single antenna systems such as envelope correlation coefficient (ECC), diversity gain (DG), total active reflection coefficient (TARC) and mean effective gain (MEG). Actually, effect of adjacent placement of antennas on overall system performance is the key factor that decides the above said parameters. However, UWB MIMO systems suffers from a major drawback of strong mutual coupling between adjacent antenna elements which severely affects the performance of the system. Hence main demand in MIMO antenna design is of enhanced isolation between adjacent antenna elements so for good performance of MIMO antenna systems, high isolation and low correlation coefficient is must (Mak et al. 2009; Saxena et al. 2018). Various methods have been suggested by researchers to reduce mutual coupling such as floating parasitic decoupling structure (Zhang et al. 2009) and a tree like structure (Srivastava and Mohan 2015) to enhance wide-band isolation.

✉ Mukesh Kumar Khandelwal
mukesh.khandelwal89@ieee.org

Sandeep Sharma
sharmadce@yahoo.co.in

Mainuddin
mainuddin@jmi.ac.in

Binod Kumar Kanaujia
bkkanaujia@yahoo.co.in

¹ Jamia Millia Islamia, New Delhi 110025, India

² Department of Computational and Integrative Sciences,
Jawaharlal Nehru University, New Delhi, Delhi 110067, India

³ Department of Electronics and Communication Engineering,
Bhagwan Parshuram Institute of Technology, Rohini-17,
New Delhi, Delhi 110089, India

Cross-polarization is also a salient feature that should be taken into account while designing a single or MIMO system antennas. It is the polarization orthogonal to the normal polarization the antenna is meant to radiate. It should as low as possible. Over the past several years, researchers have designed multiple techniques for mutual coupling reduction and cross-polarization suppression. One such technique is using Defected Ground Structure (DGS), which involves the creation of a defect in ground plane intentionally. Specific geometrical pattern (single/periodic/apertic) is created in the ground plane of printed circuits. DGS was directly integrated with microstrip patch antenna and presented for the radiation pattern and other improvements (Khan et al. 2014). This perturbation created causes a non-uniformity and discontinuity in ground plane. A disturbance is created by DGS in the ground plane current and causes a variation in capacitive and inductive characteristics of transmission line such that multiple parameters are affected by introduction of DGS in ground plane. In recent years, the Improvement in cross-polarization characteristics of microstrip antenna using DGS has been proposed (Khandelwal et al. 2017; Khandelwal et al. 2014). Four-port MIMO antennas embedded with DGS also have been presented with diversity characteristics (Sharma et al. 2018; Kumar et al. 2019).

This work discusses a novel design of dual tapered patch supported by a similar defected ground structure which gives a wide bandwidth and a high stable gain. Finally, in next design innovation, a four element MIMO system is designed and fabricated and a parallel slits DGS pattern is introduced which gives high isolation, low correlation coefficient and suppressed cross-polarization with high gain.

2 Antenna structure and analysis

Figure 1 represents the schematics of top and bottom view of proposed antenna. Single element antenna is shown in Fig. 1a which is referred as *Ant_1* in this study. It consists of a particular Y shaped patch, loaded with two side triangular structures fed by a microstrip line of 50Ω characteristic impedance. The ground plane of the above structure is defected with a similar central shape as that of patch, shown in same figure. *Ant_1* is offering an impedance bandwidth of 6.2 GHz ranging from 22.8 to 29 GHz. *Ant_1* is also analyzed with and without DGS and triangular parasitic patches, respectively. Proposed structure without DGS and without both triangular parasitic patches is resonating at 23.9 GHz whereas it starts to offer two frequency bands at 23.9 GHz as wells as 27.5 GHz after embedding the DGS in the same structure (with DGS and without triangular parasitic patches). Thus, it is concluded

that; (1) main central structure is resonating near about 23.9 GHz, (2) with the help of DGS it also starts to resonate at 27.5 GHz including previous band, (3) triangular parasitic patches maintains the return loss level below the value of -10 dB between the frequency range of both above specified bands. *S11* characteristic of *Ant_1* and its evolutionary steps are depicted in Fig. 2.

Further, four-element structure is designed as a MIMO antenna on a common ground plane and structure is referred as *Ant_2*. Schematic of top and bottom view of *Ant_2* is displayed in Fig. 1b. *Ant_2* consists of four elements (both the patch as well as DGS of each element are same as *Ant_1*) with broadside placement of adjacent antennas with a distance d . *Ant_2* offers almost similar bandwidth of about 6 GHz ranging from 23 GHz to 29 GHz as shown in Fig. 3. It offers maximum mutual coupling from port#1 to port#2, port#3 and port#4 below the value of -25 dB, -35 dB, and -38 dB, respectively.

Moreover, three slits of width W_s , length L_{s1} , L_{s2} and L_{s3} are embedded in the ground plane of *Ant_2* at a distance W_d , respectively. After embedding the slits in the ground plane, new structure is referred as *Ant_3*. Schematic of top and bottom view of *Ant_3* is shown in Fig. 1c and the values of all the variables shown in schematic are listed in Table 1. Mutual coupling between each port is suppressed about 4 dB by embedding the slits in the ground plane while *S11* remains almost same. Simulated and measured *S*-parameter variations of *Ant_3* is shown in Fig. 4. *Ant_3* offers almost same frequency band with maximum mutual coupling of -28 dB, -36 dB, and -42 dB from port#1 to port#2, port#3, and port#4, respectively. Few *S*-parameters of *Ant_2* and *Ant_3* are observed similar to each other thus not shown in Figs. 3 and 4 to reduce the complexity of the graph. Such similar parameters are presented in following groups (1) S_{11} , S_{22} , S_{33} , S_{44} , (2) S_{12} , S_{21} , S_{23} , S_{32} , S_{34} , S_{43} , (3) S_{13} , S_{31} , S_{24} , S_{42} , S_{13} , S_{31} , and (4) S_{14} , S_{41} .

3 Result and discussion

RT-Duriod-5880 substrate of dimensions L and W with thickness $h = 0.762$ mm and relative permittivity $\epsilon_r = 2.2$ is used for the fabrication of the proposed antennas. Fabrication is done by photolithography and measurement is done by Agilent™ PNA-L series Network Analyser and Agilent™ Spectrum Analyzer. The experimental characteristics of proposed antennas are measured in Anechoic Chamber. Fabricated prototypes of proposed antennas are displayed in Fig. 5. SMA connector having ground plane of about 14 mm width and 5 mm height is used to excite the *Ant_1*, this ground plane of SMA connector is worked as a metallic reflector placed in YZ plane which reflect back the

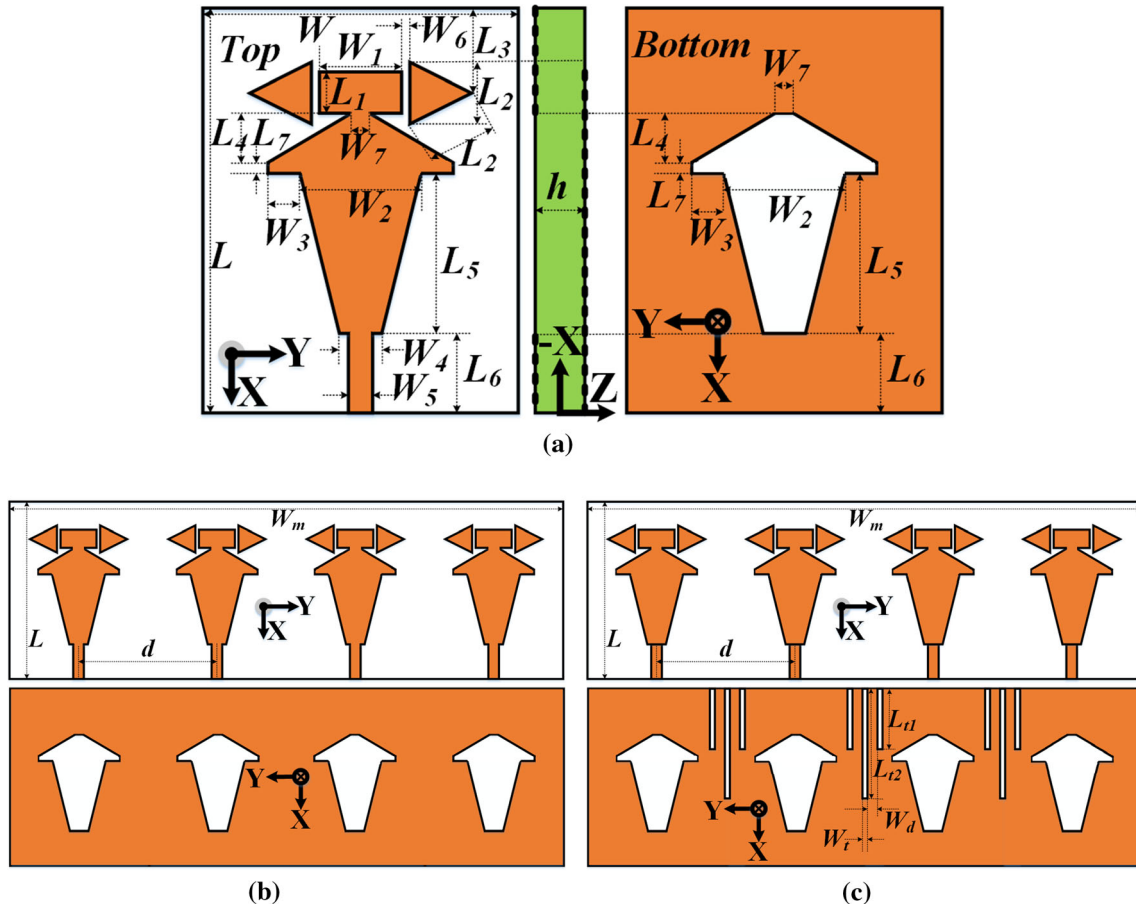


Fig. 1 Schematic of top and bottom view of proposed antenna; a *Ant_1*, b *Ant_2*, c *Ant_3*

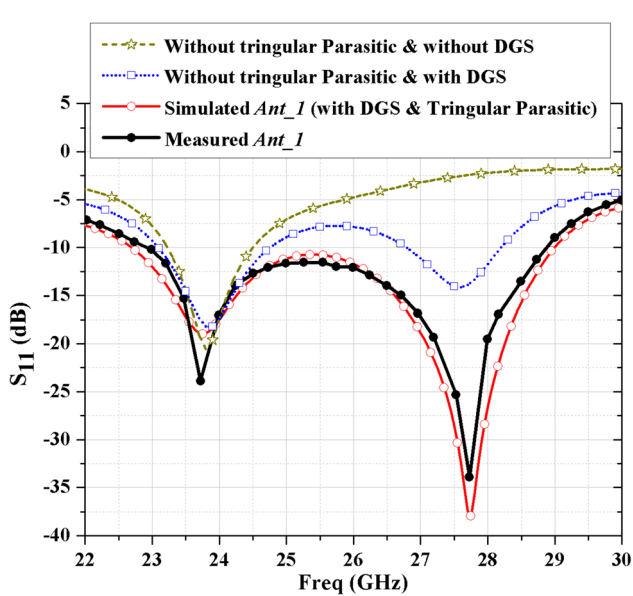


Fig. 2 Simulated and measured S_{11} variation with frequency of *Ant_1* and its evolutionary steps

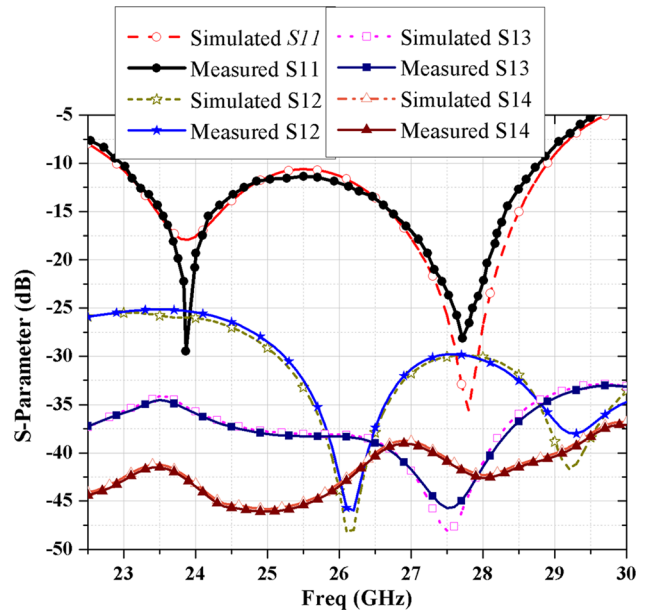
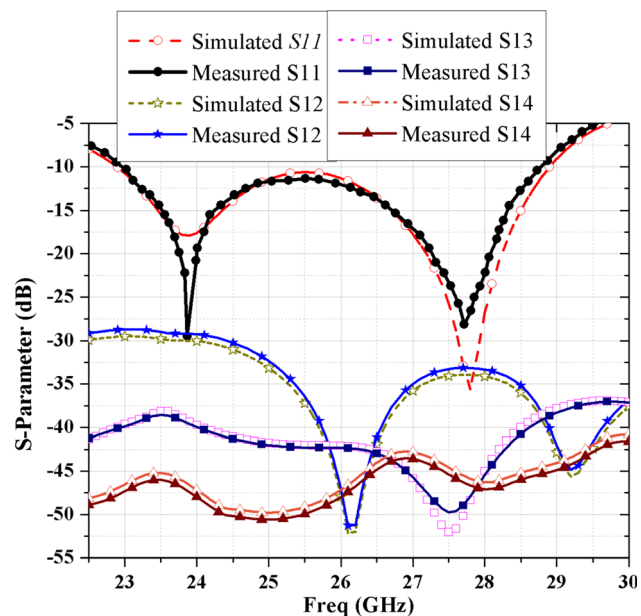
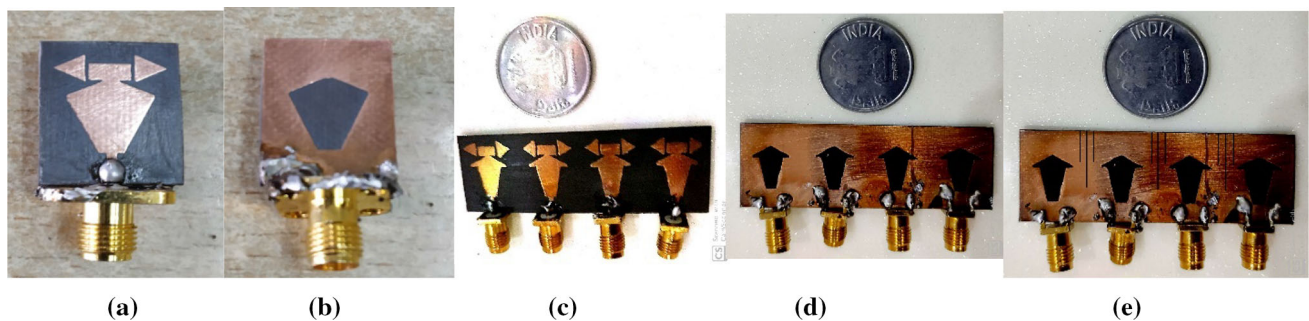


Fig. 3 Simulated and measured S-Parameter variation with frequency of *Ant_2*

Table 1 Parameter specification of proposed antenna

Parameter	Value (mm)	Parameter	Value (mm)
L	19.9	W	15
L_1	2.23	W_1	4.45
L_2	3.8	W_2	6
L_3	1.85	W_3	1.615
L_4	2.23	W_4	2.64
L_5	7.43	W_5	0.95
L_6	4.32	W_6	0.5
L_7	0.56	W_7	0.57
L_{r1}	7	L_{r2}	12
W_d	1	W_t	0.5
d	15	W_m	60

**Fig. 4** Simulated and measured S -parameter variations with frequency of Ant_3 **Fig. 5** Prototypes of fabricated antennas, **a** top view of Ant_1 , **b** bottom view of Ant_1 , **c** top view of Ant_2 (similar to Ant_3), **d** bottom view of Ant_2 , **e** bottom view of Ant_3

value of front to back ratio. Microstrip antennas with reflector also have been proposed previously in Sharma et al. (2018) and Kumar et al. (2019). On the other hand, the width of ground plane of SMA connector is reduced to the value of 5 mm with same height of 5 mm to maintain the minimum separation distance d between adjacent elements. The effect of SMA connectors are also considered in simulation of proposed structures.

Figure 6 shows the gain variation with frequency of proposed antennas in which maximum gain of about 7.3 dBi, 7.1 dBi and 7 dBi is achieved at 28.2, 28.5, and 28.6 GHz of Ant_1 , Ant_2 , and Ant_3 , respectively. After implementing MIMO elements in broadside direction, maximum gain is reduced slightly however variation between minimum and maximum values are reduced. In the operating frequency range, the gain varies from 5.1 to 7.3, 5.8 to 7.1, and 5.9 to 7 dBi of Ant_1 , Ant_2 , and Ant_3 , respectively.

The normalized radiation pattern of Ant_1 , Ant_2 , and Ant_3 are shown in Figs. 7, 8, and 9, respectively. For comparison purpose co-polar and cross-polar radiation pattern of all three antenna structures are taken at common working frequency 27.5 GHz in both major E and H planes. Cross-polarization level of all the three antennas are found below the value of -20 dB which is further suppressed by integrating DGS slits in Ant_3 .

For MIMO structure, there are few parameters of interest such as envelope correlation coefficient (ECC), diversity gain (DG), total active reflection coefficient (TARC) and mean effective gain (MEG). Envelope correlation coefficient (ECC) is a measure of the amount of correlation between adjacent antenna elements and should be zero ideally while < 0.5 practically. For the proposed MIMO antenna ECC is measured by Agilent™ PNA-L series Network Analyser and is calculated on the s -parameters without including the efficiency.

backward radiations in forward direction and enhance the

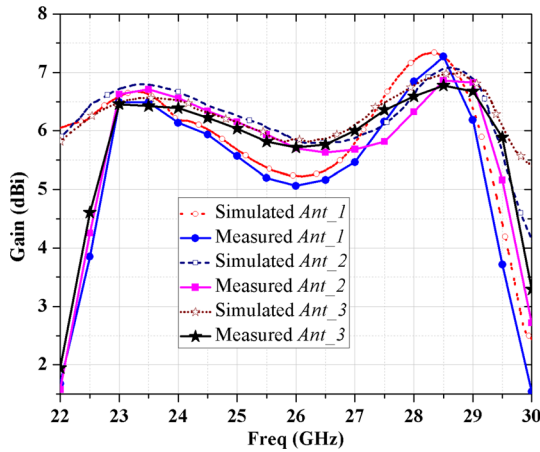


Fig. 6 Simulated and measured gain variation of proposed antenna

$$ECC = \frac{|S_{ii}^* S_{ij} + S_{ji}^* S_{jj}|^2}{(1 - |S_{ii}|^2 - |S_{ji}|^2)(1 - |S_{jj}|^2 - |S_{ij}|^2)} \quad (1)$$

Here i and j represent the respective port of the MIMO antenna.

DG describes the increase in signal to interference ratio on applying some diversity scheme. Mathematically it can be calculated using Eq. (2)

$$DG = 10\sqrt{1 - ECC^2} \quad (2)$$

As low value of ECC is a measure of high isolation between adjacent ports and is measured as less than 0.01 while DG greater than 9.95 dB for port 1 with respect to ports 2, 3 and 4 respectively as shown in Fig. 10. Similarly,

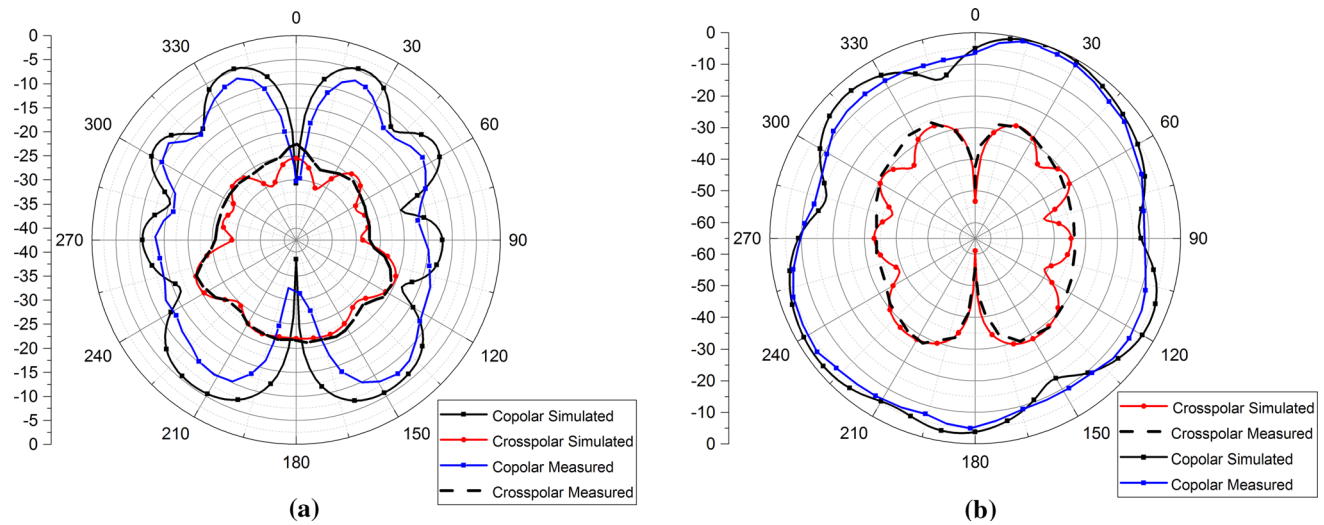


Fig. 7 Simulated and measured radiation pattern of Ant_1 at 27.5 GHz of; a E-Plane, b H-Plane

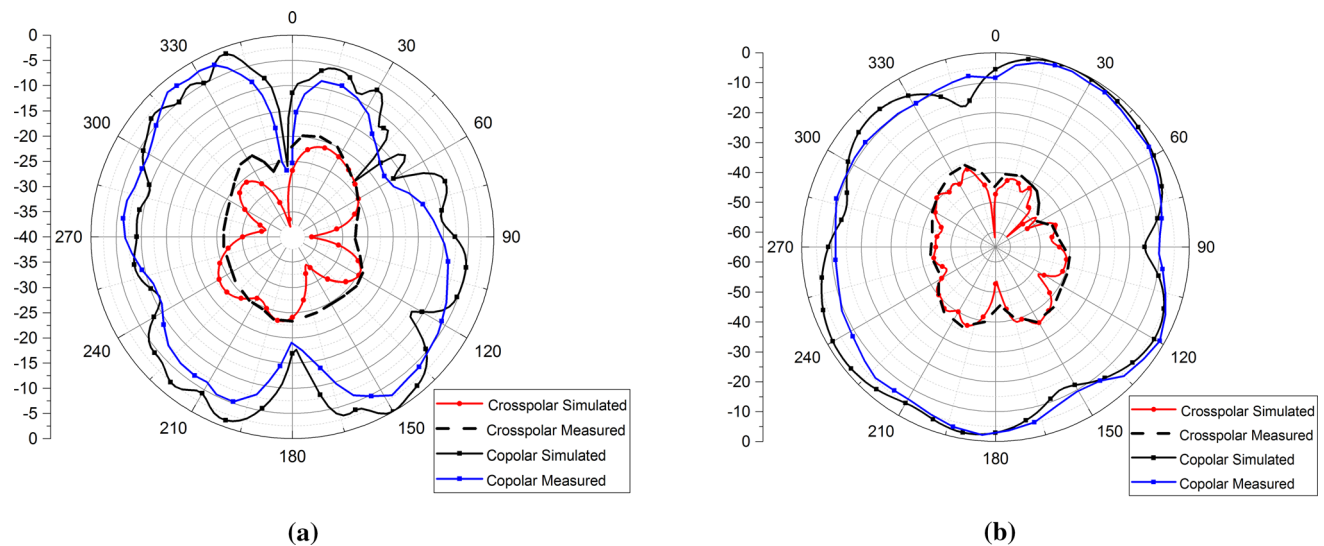


Fig. 8 Simulated and measured radiation pattern of Ant_2 at 27.5 GHz of; a E-Plane, b H-Plane

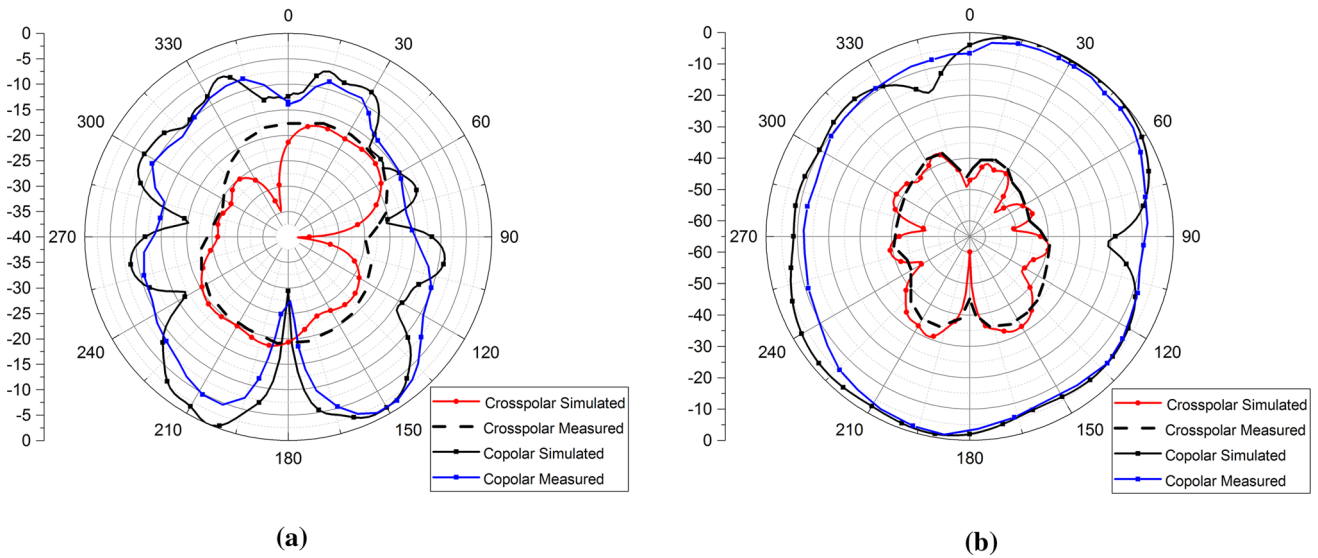


Fig. 9 Simulated and measured radiation pattern of *Ant_3* at 27.5 GHz of; **a** *E*-Plane, **b** *H*-Plane

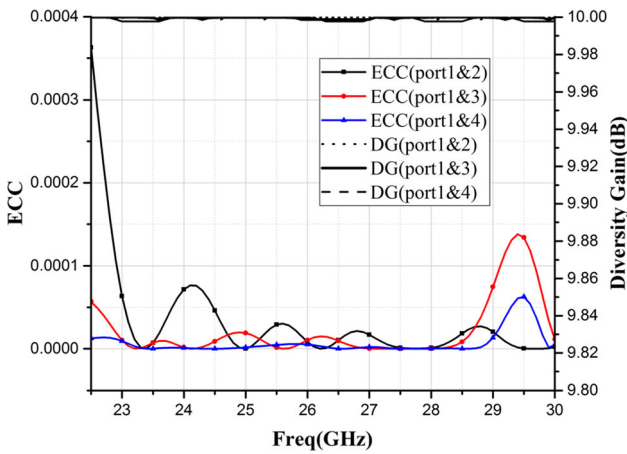


Fig. 10 Measured ECC and DG for port 1 of *Ant_3*

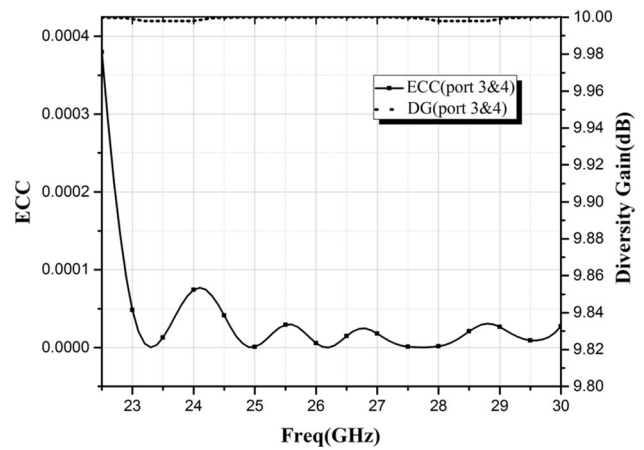


Fig. 12 Measured ECC and DG for port 3 of *Ant_3*

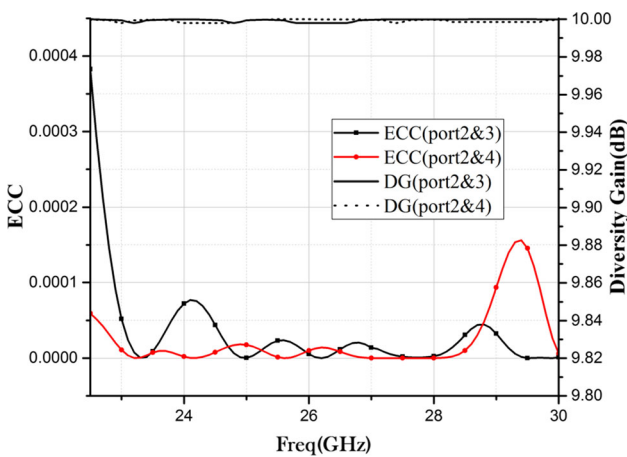


Fig. 11 Measured ECC and DG for port 2of *Ant_3* for port 2 with respect to ports 3 and 4 as well as for port 3

with respect to port 4 are shown in Figs. 11 and 12, respectively.

MEG is a measure of relative mean power levels between signals transmitted from each antenna. Actually, it gives the average power received by test antenna to the sum of average powers that would have been received using two isotropic radiators, vertically and horizontally polarized respectively. The MEG can be calculated using Eq. (3)

$$MEG = \iint_{00}^{2\pi\pi} \left\{ \frac{XPR}{1 + XPR} G_{\theta}(\theta, \phi) P_{\theta}(\theta, \phi) + \frac{1}{1 + XPR} G_{\phi}(\theta, \phi) P_{\phi}(\theta, \phi) \right\} \sin \theta d\theta d\phi \quad (3)$$

Here XPR represents the cross-polarization power ratio and G_{θ} , G_{ϕ} , P_{θ} and P_{ϕ} are the elevation and azimuth components of antenna power gain patterns and angular

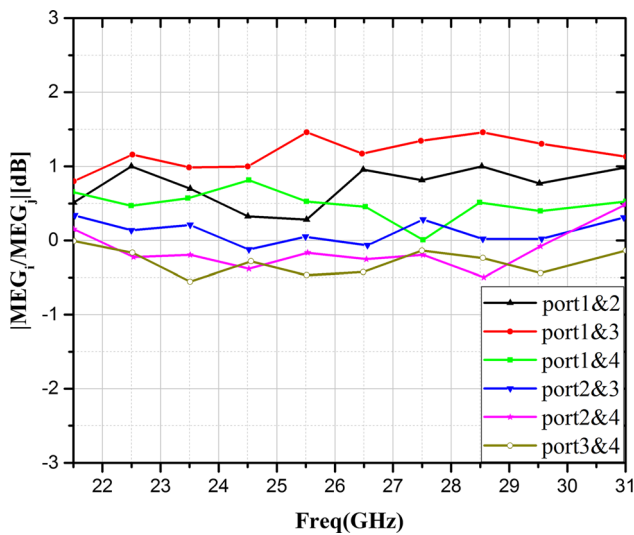


Fig. 13 Ratio of MEGs of every two-antenna element for the proposed MIMO antenna

diversity of incident power respectively. The practical value of ratio $|MEGi/MEGj|$ should be $< \pm 3$ dB, where i and j are antenna elements, and the ratio of MEGs of two antenna elements versus frequency lies in permissible range as shown in Fig. 13.

TARC is given by square root of the ratio of the difference of total available power and the radiated power to total available power as given by Eq. (4)

$$TARC = \sqrt{\frac{\text{availablepower} - \text{radiatedpower}}{\text{availablepower}}} \quad (4)$$

The practical value of TARC always lies between 0 and 1 which means less than 0 dB. It is mainly used to observe

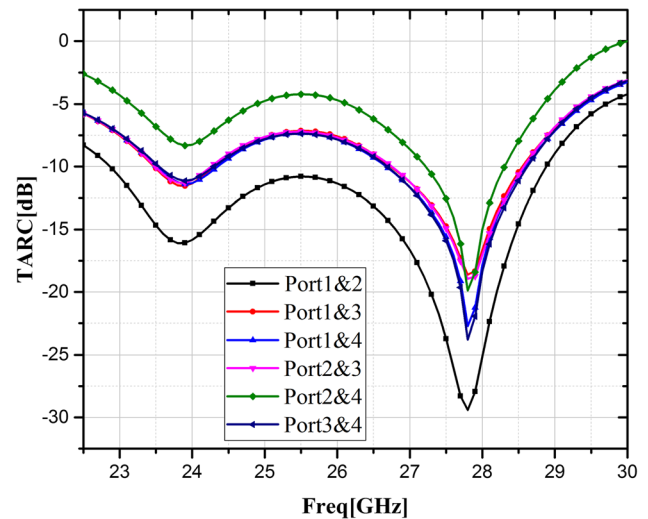


Fig. 14 TARC versus frequency for the proposed MIMO antenna

the effective return loss of the MIMO system. The mathematical expression of TARC is given by Eq. (5)

$$TARC = \sqrt{\frac{(S_{ii} + S_{ij})^2 + (S_{ji} + S_{jj})^2}{2}} \quad (5)$$

The variation of TARC versus frequency for proposed MIMO antenna *Ant_3* is represented by Fig. 14 and it is observed that it is mostly less than -5 dB.

A comparison analysis of proposed antenna *Ant_3* with similar literature is presented in Table 2 and it is analyzed that proposed antenna offers better characteristics in terms of compactness, minimum mutual coupling, higher gain and low cross-polarization level with best diversity conditions among all the four ports.

Table 2 Comparison of proposed and earlier reported antennas

References	Size (mm ²)	Operating range (GHz)	Mutual coupling (dB)	Gain (dBi)	Cross-polarization
Zhang et al. (2009)	35 × 40	3.1–10.6	− 16	3.1	–
Srivastava and Mohan (2015)	27 × 28	3–10.6	− 16	3	–
Ren et al. (2014)	32 × 32	3.1–10.6	− 15	1.7–4.2	–
Liu et al. (2013)	26 × 40	3.1–10.6	− 15	0.9–6.5	–
Deng et al. (2016)	30 × 40	3–10.6	− 16	–	High
Zhang et al. (2015)	26 × 26	3.1–10.6	− 15	0.85	–
Kumar (2016)	31 × 20	3.8–7.8	− 15	–	–
Lee et al. (2012)	55 × 13.5	1.85–11.9	− 17.2	4.96	–
Chacko et al. (2013)	50 × 50	2.76–10.75	− 15	2.8	Moderate
Gao et al. (2014)	48 × 48	2.5–12	− 18	3	–
Proposed	19.9 × 60	23–29	− 28	7.1	Low

4 Conclusion

Four-element MIMO antenna is successfully designed and analyzed. Proposed antenna is operating from 23 to 29 GHz and offers better radiation characteristics with suppressed cross-polarization below the value of -20 dB within the whole operating band. A maximum gain of 7.1 dBi is noticed at 28.8 GHz whereas mutual coupling is achieved below the value of -28 dB. Further, diversity characteristics are verified in terms of ECC, DG, TARC and ratio of MEG which lie within the specified limit for a MIMO antenna. All the simulated results are verified by experimental measured results and both results are found in good agreement.

References

- Chacko BP, Augustin G, Denidni TA (2013) Uniplanar polarization diversity Antenna for ultrawideband systems. *IET Microw Antennas Propag* 7(10):851–857
- Deng J-Y, Guo L-X, Liu X-L (2016) An ultrawideband MIMO Antenna with a high isolation. *IEEE Antenna Wirel Propag Lett* 15:182–185
- Gao P, He S, Wei X, Xu Z, Wang N, Zheng Y (2014) Compact printed UWB diversity slot Antenna with 5.5-GHz band-notched characteristics. *IEEE Antennas Wirel Propag Lett* 13:376–379
- Kaiser T, Zheng F, Dimitrov E (2009) An overview of ultrawide band systems with MIMO. *Proc IEEE* 2(2):285–312
- Khan MS et al (2014) Compact ultrawide band diversity antenna with a floating parasitic digitated decoupling structure. *Microw Antennas Propag* 8(10):747–753
- Khandelwal MK, Kanaujia BK, Dwari S, Kumar S (2014) Bandwidth enhancement and cross-polarization suppression in ultra-wide-band microstrip antenna with defected ground plane. *Microw Opt Technol Lett* 56(9):2141–2146
- Khandelwal MK, Kanaujia BK, Kumar S (2017) Defected ground structure: fundamentals, analysis, and applications in modern wireless trends. *Int J Antennas Propag* 2017:22. <https://doi.org/10.1155/2017/2018527>
- Kumar J (2016) Compact MIMO antenna. *Microw Opt Technol Lett* 58(6):1294–1298
- Kumar A, Rai CS, Khandelwal MK, Kanaujia BK (2019) Low envelope correlation coefficient, enhanced gain, and suppressed mutual coupling in compact 4-port MIMO microstrip antenna loaded with metasurface. *Microsyst Technol*. <https://doi.org/10.1007/s00542-019-04513-0>
- Lee J-M, Kim K-B, Ryu H-K, Woo J-M (2012) A compact ultrawideband MIMO Antenna with WLAN band-rejected operation for mobile devices. *IEEE Antennas Wirel Propag Lett* 11:990–993
- Liu L, Cheung SW, Yuk TI (2013) Compact MIMO Antenna for portable devices in UWB applications. *IEEE Trans Antennas Propag* 61(8):4257–4264
- Mak ACK, Rowell CR, Murch RD (2009) Isolation enhancement between two closely packed antennas. *IEEE Trans Antennas Propag Lett* 8:209–211
- Ren J, Hu W, Yin Y, Fan R (2014) Compact printed MIMO Antenna for UWB applications. *IEEE Antenna Wirel Propag Lett* 13:1517–1520
- Saxena S, Kanaujia BK, Dwari S, Kumar S, Tiwari R (2018) MIMO antenna with built-in circular shaped isolator for sub-6 GHz 5G applications. *Electron Lett* 54(8):478–480
- Sharma S, Mainuddin, Kanaujia BK, Khandelwal MK (2018) Design of 4-element microstrip array of wideband reflector antenna with stable high gain characteristics. *Microsyst Technol*. <https://doi.org/10.1007/s00542-018-4189-3>
- Srivastava G, Mohan A (2015) Compact dual-polarized UWB diversity antenna. *Microw Opt Technol Lett* 57(12):2951–2955
- Wallace J, Jensen M, Swindlehurst A, Jeffs B (2003) Experimental characterization of the MIMO wireless channel: data acquisition and analysis. *IEEE Trans Wirel Commun* 2(2):335–343
- Wang X, Feng ZH, Luk KM (2009) Pattern and polarization diversity antenna with high isolation for portable wireless devices. *IEEE Antennas Wirel Propag Lett* 8:209–211
- Zhang S, Ying Z, Xiong J, He S (2009) Ultrawideband MIMO/diversity antennas with a tree-like structure to enhance wideband isolation. *IEEE Antenna Wirel Propag Lett* 8:1279–1282
- Zhang J-Y, Zhang F, Tian W-P, Luo Y-L (2015) ACS-fed UWB-MIMO Antenna with shared radiator. *Electron Lett* 51(17):1301–1302

Publisher's Note Springer Nature remains neutral with regard to jurisdictional claims in published maps and institutional affiliations.